A Short Review on the Magnetic Effects Occurring at Organic Ferromagnetic Interfaces Formed between Benzene-Like Molecules and Graphene with Ferromagnetic Surfaces

Nicolae Atodiresei[a], Vasile Caciuc[a], and Predrag Lazić[b]

[a] Peter Grünberg Institut (PGI-1) and Institute of Advanced Simulation (IAS-1), Forschungszentrum Jülich and JARA, 52425 Jülich, Germany

[b] Rudjer Boskovic Institut, Zagreb 10000, Croatia

Reprint requests to N. A.; E-mail: n.atodiresei@fz-juelich.de

Z. Naturforsch. **69a**, 360 – 370 (2014) / DOI: 10.5560/ZNA.2014-0026
Received January 15, 2014 / revised February 28, 2014 / published online July 15, 2014

This paper is dedicated to Professor Jörg Fleischhauer on the occasion of his 75th birthday.

In this article, we briefly summarize our results gained from recent density functional theory simulations aimed to investigate the interaction between organic materials containing π-electrons (i. e., several benzene-like molecules and graphene) with ferromagnetic surfaces. We show how the strong hybridization between the p_z-electrons that initially form the π molecular orbitals with the magnetic d-states of the metal influences the spin polarization, the magnetic exchange coupling, and the magnetization direction at hybrid organic–ferromagnetic interface. From a practical perspective, these properties play a very important role for device applications based on organic materials and magnetic surfaces.

Key words: Density Functional Theory; Ab Initio Studies; Molecular Electronics; Molecular Spintronics; Spin-Polarization; Magnetic Exchange Coupling; Hybrid Interface; Bonding Mechanism.

1. Introduction

The target of molecular electronics [1] is to employ organic molecules as functional units in electronic devices, i. e., as molecular wires [2], diodes [3], molecular switches [4], and transistor-like devices [5]. In practice, these devices rely on the electron charge degree of freedom by manipulating the electronic properties of the hybrid molecule–substrate system. Furthermore, the prospect of integrating the electron spin degree of freedom into molecular-based electronic devices leads to the emerging field of molecular spintronics [6].

An example of a molecular spintronic device is the organic spin valve [7] that consists of a layered structure of two ferromagnetic electrodes separated by an organic spacer used to magnetically decouple the two electrodes. The high performance of such devices relies on the spin injection into and the spin transport throughout the organic material. Therefore, one of the most important issues that must be addressed is the efficiency of the spin injection and spin transport in hybrid organic–magnetic systems [8, 9]. As a consequence, it is crucial to understand the role of the interface hybrid states in manipulating the magnetic properties at the interface and, in particular, to overcome the spin-information loss in spintronic devices [10]. Within this context, the technological steps in future molecular spintronics aim to

(i) implement specific spin-dependent functions within single molecular building blocks and
(ii) use organic molecules to tune the magnetic properties of underlying magnetic substrates.

For example, it has been demonstrated that the supramolecular spin-valve devices [11] can successfully incorporate the properties of the single molecule magnets [12]. In addition, recent studies showed that the adsorption of magnetic or non-magnetic organic materials onto a magnetic surface could be used to manipulate the spin-filter properties of the hybrid organic–metal interface [13 – 15]. Moreover, the flat adsorption of organic molecules based on phenalenyl-type radicals onto ferromagnetic metals modifies the magnetic exchange couplings between the surface

magnetic atoms and proved to be a viable approach in constructing building blocks for future molecular-scale quantum spin memory devices and processors [6].

To summarize, the success of future molecular spintronics devices relies on two important parameters that determine the performance of such devices:

(i) the spin-dependent electronic structure responsible for the injected spin polarized current from the hybrid interface and
(ii) the change of the magnetic properties of the surface metal atoms (i. e., magnetic exchange interaction and the spatial direction of the magnetic moments) due to their interaction with the organic material.

However, although significant advances have been reported in the recent years in the field of molecular spintronics, fundamental theoretical studies are still necessary to achieve a basic understanding on how to design and control the spin-based molecular electronic devices. In particular, in this short review we will analyze how to control the magnetic properties of hybrid organic–magnetic interfaces by manipulating the interaction between the π-conjugated organic materials and the magnetic surfaces.

1.1. Physisorption and Chemisorption Bonding Mechanisms

Ideally, the adsorption of a molecule onto a metal surface could be described by two bonding mechanisms:

(i) physisorption or
(ii) chemisorption.

A general scheme illustrating basic aspects displayed by the two physisorption and chemisorption bonding mechanisms is depicted in Figure 1. However, in real molecular–metal systems these two processes can coexist. As a consequence, for some specific combined molecule–metal systems the bonding mechanism is mostly dominated by physisorption while in other hybrid molecular–metallic systems the chemisorption bonding mechanism is predominant. Furthermore, a charge transfer between the molecule and the surface can take place that leads to an additional electrostatic component of the binding in the case of physisorption or a strong polar covalent character of the binding in the case of chemisorption.

The strength of the molecule–surface interaction is quantitatively described by the adsorption energy E_{ads}. This is defined as $E_{ads} = E_{system} - (E_{surface} +$

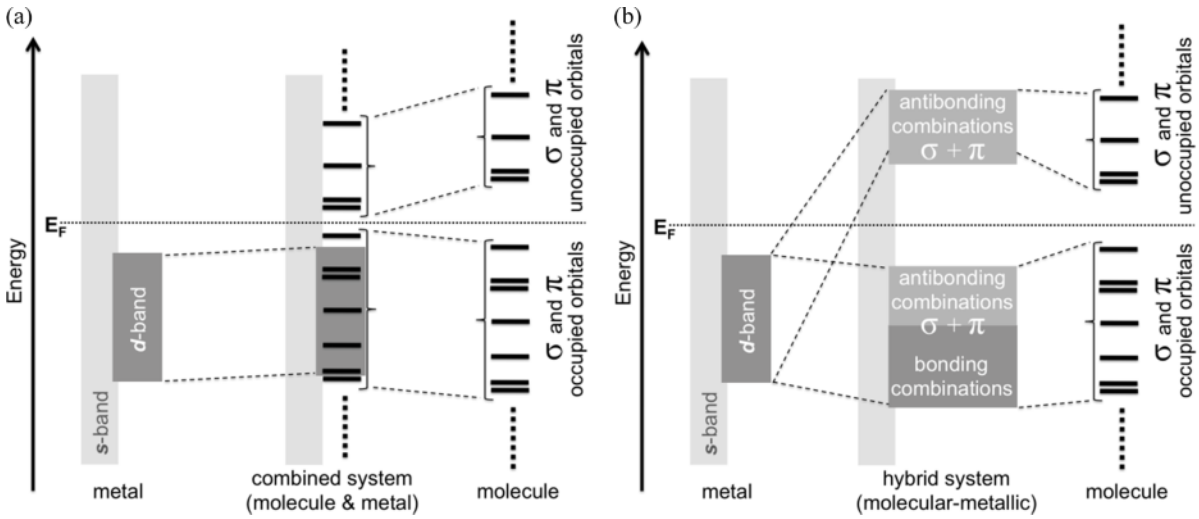

Fig. 1. A general scheme illustrating the energy level alignment as a result of the interaction between an organic molecule with a metallic surface. (a) The physisorption bonding mechanism characterizes a week molecule–metal interaction and leads to a renormalization of the HOMO–LUMO gap in molecule due to polarization effects [16, 17]. (b) The chemisorption bonding mechanism is the consequence of a strong molecule–metal interaction when the atomic type orbitals that initially form the molecular orbitals hybridize with the metallic bands leading to bonding and antibonding hybrid bands with mixed molecular–metal character.

E_{molecule}), where E_{system} is the total energy of the molecule–surface system while E_{surface} and E_{molecule} denote the total energy of the clean surface and that of the molecule in the gas phase, respectively.

Overall, both physisorption and chemisorption type interactions lead to changes of molecule and metal electronic structures due to their mutual interaction. As a general characteristic, the physisorption bonding mechanism is driven by the long-range attractive van der Waals (vdW) forces [18] and does not lead to a significant change of the gas-phase electronic structure of the molecule and the surface (see Fig. 1a). In this case, the molecular orbitals (MOs) represent still a meaningful concept and can be safely used to describe the electronic structure of the molecule. Nevertheless, it is important to note that the physisorption process leads to a renormalization of the highest occupied molecular orbital (HOMO)-lowest unoccupied molecilar orbital (LUMO) gap due to molecule–surface image potential interaction [16, 17]. The weak molecule–surface interaction responsible for physisorption is characterized by a small adsorption energy with an upper value of ~ 0.1 eV and a molecule–substrate distance larger than 3 Å [18].

The chemisorption bonding mechanism leads to the creation of a new quantum mechanical system as a result of the strong hybridization between the atomic type orbitals that initially form the molecular orbitals with the metallic states. From this perspective, the hybridization implies the formation of bonding and antibonding electronic states as a linear combination of atomic orbitals similar to the molecular orbitals as described by the molecular orbital theory [19].

These new bonding and antibonding hybrid bands (see Fig. 1b) have a mixed molecular–metal character and some of them do not resemble any of the states of the separated molecule and substrate [13, 20, 21]. The strong molecule–surface interaction that leads to chemisorption is characterized by a large adsorption energy with a lower value of ~ 0.5 eV and a molecule–substrate distance below 2.5 Å [22].

1.2. Theoretical Tools

Nowadays, one of the most used theoretical instruments employed to study the geometrical, electronic, and magnetic properties of materials containing hundreds and even thousands atoms is the density func-

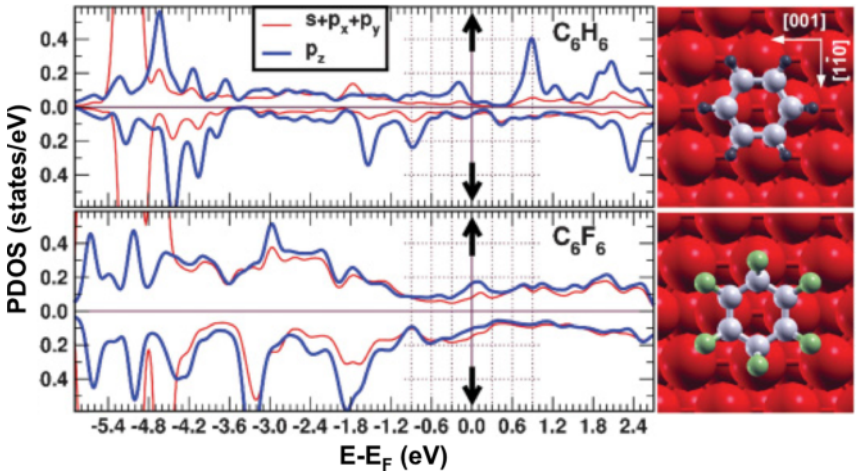

Fig. 2 (colour online). The spin-resolved projected local density of states (PDOS) of the C_6X_6 (X=H,F) molecules adsorbed on the 2ML Fe/W(110) ferromagnetic surface shows broad molecular–metallic states due to the hybridization between the atomic type orbitals that initially form the molecular orbitals with the ferromagnetic metallic bands. The black arrows indicate the spin-up and spin-down channels. A top view of the adsorption geometry for each molecule is shown in the right side of the figure (color of the atoms C-gray, H-dark gray, F-green and Fe-red). Note that a strong hybridization occurs mostly between the out-of-plane orbitals (i. e., p_z of C and Fe d-orbitals with a z-component as d_{z^2}, d_{xz}, and d_{yz}) while the in-plane orbitals are weakly interacting (i. e., s, p_xp_y of C and Fe d-orbitals as $d_{x^2-y^2}$ and d_{xy}). The DOS of both adsorbed molecules shows an energy-dependent spin polarization implying that in a specific energy interval the number of spin-up and spin-down states is different and, as a consequence, the molecule has a net magnetization density that can be measured as a spin-contrast in SP-STM experiments [13, 14]. Reprinted with permission from [34]. Copyright 2011 IOP Publishing Ltd.

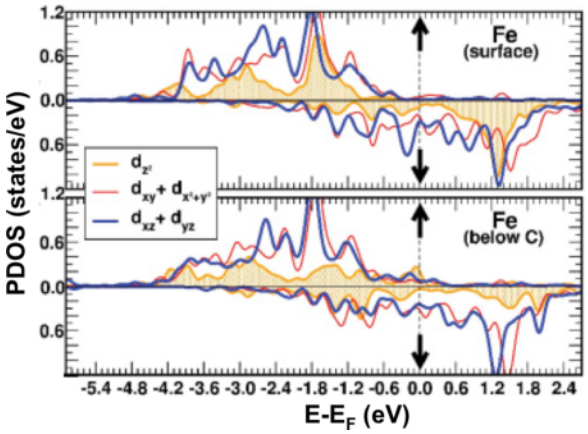

Fig. 3 (colour online). The spin-resolved local projected density of states (PDOS) of an Fe atom of the clean surface (upper panel), an Fe atom below a C–C bond (lower panel) of the C_6H_6 molecule indicates that the majority of electrons are in the spin-up channel while the minority electrons are in the spin-down channel [14, 34]. The black arrows indicate the spin-up and spin-down channels. Reprinted with permission from [34]. Copyright 2011 IOP Publishing Ltd.

tional theory (DFT) [23]. Although this theoretical approach is, in principle, exact for the ground-state properties of any system, in practical simulations the DFT accuracy strongly depends on the approximation used to describe the exchange-correlation functional (i. e. local density approximation (LDA) [24], generalized gradient approximation (GGA) [25], and van der Waals density functional (vdW-DF) [26]).

At this point we note that the structures of the chemisorbed molecular systems are in general correctly described by the GGA type functionals, although the calculated adsorption energies might not be always chemically accurate [27, 28].

Nevertheless, for the physisorbed molecular systems the semi-local GGA type exchange-correlation functionals have a significant limitation since they cannot describe the long-ranged attractive van der Waals (vdW) interactions such that even the geometry of vdW-bonded systems is not correctly reproduced [18, 26]. A simple way to include the vdW effects in DFT is to use a combination of GGA and a semi-empirical vdW approach [29] while another way to incorporate the dispersion interactions in DFT is to employ a functional that explicitly includes the non-local correlation effects [26]. Each of these possibilities to account for the missing vdW interaction has its advantages or disadvantages [18, 29, 30] and by using both of these methods we can achieve thorough understanding of the hybrid organic material–metal system [31, 32].

1.3. Organic Materials Adsorbed on Ferromagnetic Surfaces

In Section 1.1 we shortly stated that a weak interaction between the molecule and the surface leads to a physisorption while the chemisorption implies a strong interaction that gives rise to a new hybrid material with both organic and metallic characteristics. Due to the hybridization effects, the electronic and magnetic properties of the hybrid organo–metallic system will differ in most cases from those of the separated parts, i. e., organic material and metal surface. Depending on the metal reactivity, in some combined molecule–metal systems the bonding mechanism is governed by physisorption while for other hybrid molecular–metallic systems the binding is driven by chemisorption [33]. Interestingly, for organic materials with a large spatial extend as graphene nanoflakes adsorbed on the Ir(111) and Co/Ir(111) surfaces, the physisorption and chemisorption processes can be present independently in different regions within the same organic–metal system [15, 32]. Even more, in both physisorption and chemisorption bonding mechanisms an additional charge transfer between organic material and metal surface can take place that further leads to an electrostatic component in the binding for the physisorption or strong polar covalent type bonds in the case of chemisorption [13, 15].

In the next paragraphs, we will summarize several recent studies performed in our group that demonstrate how by adsorbing π-conjugated organic materials onto ferromagnetic metal surfaces, the magnetic properties of the hybrid organic–metallic system can be specifically tuned by the strength of the organic material–metal interaction. This can be achieved by

(i) chemically functionalizing the adsorbed organic molecules or
(ii) an appropriate choice of the metal substrate and
(iii) in the case of extended systems as graphene by modulating the specific organic–surface interaction using the lattice mismatch of the layered materials.

As a first example, we consider the adsorption of the hydrogenated and fluorinated benzene molecules (C_6X_6, X=H, F) onto a ferromagnetic surface contain-

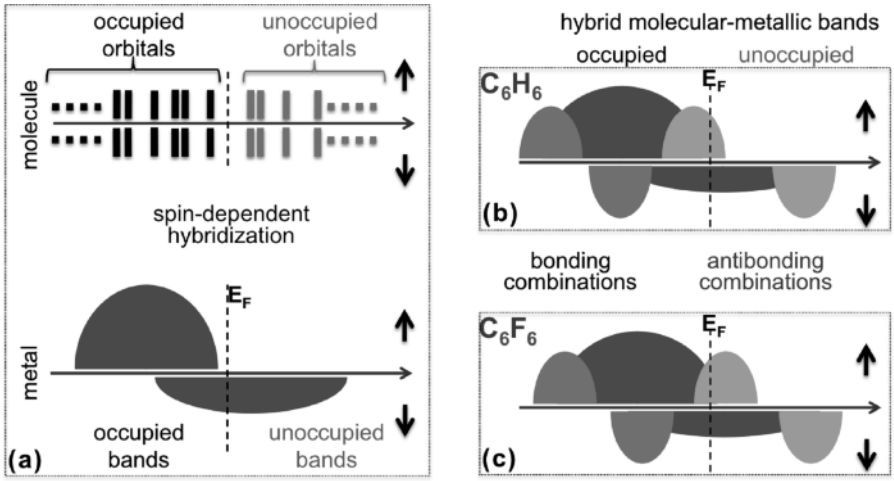

Fig. 4. Cartoon illustrating the interaction between non-magnetic organic molecules and ferromagnetic surfaces. (a) Schematic drawings of the molecular orbitals (upper panel) and *d*-states of the ferromagnetic substrate (lower panel). The small black arrows indicate the spin-up and spin-down channels. The spin-dependent hybridization leads to the formation of bonding hybrid molecular–metallic states that appear at low energies well below the Fermi level in both spin-up and spin-down channels. The antibonding hybrid molecular-metallic states are located in an energy window around the Fermi energy for the spin-up channel and above the Fermi energy for the spin-down channel. Most of the hybrid antibonding bands are situated below the Fermi energy for the C_6H_6 molecule (b) (see also the spin-up states in the upper panel of Fig. 2) while for the C_6F_6 molecule (c) most of these antibonding bands are shifted just above the Fermi energy (see also the spin-up states in the lower panel of Fig. 2).

ing two monolayers of iron on W(110) that we will further denote as 2ML Fe/W(110). The energetic position of the σ- and π-orbitals in the molecules can be manipulated by a substitution of the hydrogen in the benzene molecule with more electronegative atoms as fluorine that has a strong electron withdrawing effect. In molecular electronics and spintronics this process that is often referred as chemical functionalization [34, 35].

One of the most important consequences of the chemical functionalization is that the molecule–surface binding strength can be finely adjusted [31, 34] due to the different hybridization of the atomic type orbitals that initially form the σ- and π-molecular orbitals with the *d*-states of the metallic surface. More specifically, in the case of the fluorinated benzene (C_6F_6) the π-conjugation is decreased with respect to the hydrogenated molecule (C_6H_6), which in turn leads to a weaker molecule–surface interaction. Indeed, the adsorption energy of the C_6F_6 onto the ferromagnetic 2ML Fe/W(110) substrate amounts to 0.362 eV while the benzene (C_6H_6) binds more strongly to this metallic surface with an adsorption energy of 0.978 eV.

A detailed picture of the binding mechanism occurring between the C_6H_6 and C_6F_6 with the ferromagnetic surface can be inferred from the analysis of the spin-resolved projected local density of states (PDOS) for our hybrid molecular–metallic systems shown in Figures 2 and 3. A very important aspect that we would like to emphasize is that upon adsorption a spin-dependent hybridization will occur mostly between the p_z-atomic type orbitals that originally form the π-molecular orbitals and the out-of-plane *d*-states (i. e., the d_{xz}, d_{yz}, d_{Z^2} orbitals containing *z*-component) of the ferromagnetic iron atoms. As schematically shown in Figure 1b this hybridization leads to the formation of new molecule–metal hybrid bands with bonding and antibonding character specific for each spin-channel [13, 14].

As depicted in Figure 2, in the spin-up channel hybrid organic–metallic bonding states are situated at low energies while the antibonding combinations of the molecule–surface orbitals appear in an energy window situated around the Fermi energy. More precisely, few of these antibonding combinations are occupied and situated below Fermi energy, while some other antibonding combinations are unoccupied and situated above the Fermi energy. We note also that at clean metal sites the states with large weight around the Fermi level are present only in the spin-down chan-

nel. Furthermore, Figure 3 shows that as a result of the strong hybridization between the Fe with the C atoms, the shapes of the out-of-plane d-states are changed with respect to those of the clean surface Fe atoms. In addition, the magnetic moments of the iron atoms (e. g. $+2.47\mu_B$) binding directly to the carbon atoms are decreased as compared to the clean surface magnetic atoms (e. g. $+2.82\mu_B$) [14, 34].

A very important feature is that upon adsorption on the ferromagnetic 2ML Fe/W(110) the benzene (hydrogenated) molecule acquires a very small magnetic moment (e. g. $-0.076\mu_B$) that practically can be neglected. In contrast, the adsorbed fluorinated benzene molecule has a quite large magnetic moment (e. g. $-0.278\mu_B$) oriented antiferromagnetically with respect to the iron substrate. It is interesting to note that the magnetic moment induced in the π-type orbitals at the molecule site correlates with the electron affinity of the substituent, i. e., by increasing the substituent electronegativity when going from hydrogen to an iron atom the molecular magnetic moment also increases. An additional observation is that for the benzene molecule the hybrid antibonding states are located mostly below the Fermi level, while for the fluorinated benzene these antibonding orbitals are emptied, i. e., most of them are pushed above the Fermi energy (see Fig. 2 and also the schematic views presented in Fig. 4).

The mechanism explaining the spin-dependent hybridization occurring at the organic–ferromagnetic interface is conceptually similar to the p_z–d Zener exchange mechanism [36] and is schematically depicted in Figure 4 for both C_6H_6 and C_6F_6 molecule–magnetic metal systems. At this point we would like to remind the generality of such Zener-type exchange mechanisms that are successfully employed to describe the interaction of π-conjugated organic molecules with ferromagnetic atoms as lanthanides which electronic structure resembles a π–f Zener exchange mechanism [37, 38].

1.4. Spin Polarization Above the Hybrid Organic–Ferromagnetic Interface

As already discussed above in Figure 2 and schematically shown in Figure 4, the spin-resolved

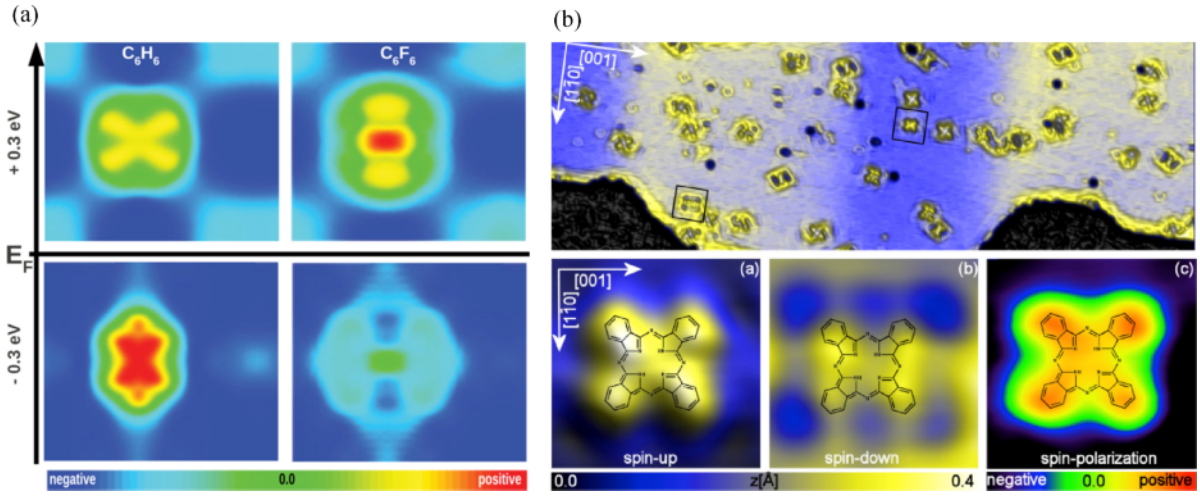

Fig. 5 (colour online). (a) Simulated spin polarization above the C_6X_6 (X=H,F) molecule adsorbed on the 2ML Fe/W(110) surface for energy intervals below (occupied, $[E_F - 0.3]$ eV) and above (unoccupied, $[E_F + 0.3]$ eV) the Fermi level. Interestingly, an inversion of the spin polarization with respect to the ferromagnetic substrate for energy intervals below and above the Fermi energy is present in the case of adsorbed C_6H_6 molecule. The adsorbed C_6F_6 molecule shows an inversion of the spin polarization with respect to the ferromagnetic substrate only for energy intervals above the Fermi level and preserves the spin polarization of the iron ferromagnetic surface for energy intervals below the Fermi level. (b) A spin-polarized scanning tunneling microscopy (SP-STM) overview image (upper panel) of a multidomain (blue/yellow) 2ML Fe/W(110) ferromagnetic surface containing phthalocynanine (H_2Pc) molecules (lower panel). The high-resolution SP-STM images for both spin-up and spin-down channels and the local spin polarization for an adsorbed H_2Pc molecule. Note that the molecule shows a high, locally varying spin polarization ranging from attenuation to inversion with respect to the ferromagnetic Fe film. (a) Reprinted with permission from [34]. Copyright 2011 IOP Publishing Ltd. (b) Reprinted with permission from [14]. Copyright 2010 IOP Publishing Ltd.

PDOS of the adsorbed benzene and fluorinated benzene molecules reveals a very fascinating feature: the energy dependent spin polarization[1]. This implies that for a specific energy interval the number of spin-up and spin-down states is unbalanced. As a consequence, for that specific energetic interval the molecule has a net magnetization density delocalized over the molecular plane.

In the case of the adsorbed benzene molecule onto the 2ML Fe/W(110) surface, for energy intervals around the Fermi level, the spin-up states have a large weight at the molecular site, while on the clean ferromagnetic surface the spin-down states are predominant. Therefore, with respect to the ferromagnetic surface an inversion of the spin polarization take place at the molecular site for energy intervals below and above the Fermi level [13, 14]. Interestingly, this is not the case for the adsorbed fluorinated molecule where the spin polarization below the Fermi level is the same as on the ferromagnetic substrate while the inversion of the spin polarization occurs only for energy intervals above the Fermi energy [13]. These aspects are clearly visualized in Figure 5a, which presents the simulated spin polarization maps 3.0 Å above the molecular site for the energy intervals below ($[-0.3, 0.0]$ eV) and above ($[0.0, +0.3]$ eV) the Fermi level.

Furthermore, our density functional theory investigations showed that by an appropriate chemical functionalization of organic molecules adsorbed onto a ferromagnetic surface, we can

(i) induce a magnetic molecule at the molecular site and
(ii) tailor the spin-unbalanced electronic structure above the adsorbed molecules.

Besides this, our theoretical simulations indicate the importance of interface hybrid organic–metallic states rather than the molecular magnetic moment on the spin polarization.

The validity of the theory driven concepts was demonstrated by performing spin-polarized scanning tunneling microscopy (SP-STM) experiments [39, 40] on the phthalocyanine (H_2Pc) [14] and Co-phthalocyanine molecules (CoPc) [13] adsorbed onto the 2ML Fe/W(110) substrate. These SP-STM mea-

[1] Note that the spin polarization is defined as $n^{\Uparrow} - n^{\Downarrow})/(n^{\Uparrow} + n^{\Downarrow})$, where the $n^{\Uparrow}$ and $n^{\Downarrow}$ represent the spin-up and spin-down charges integrated over a specific energy interval.

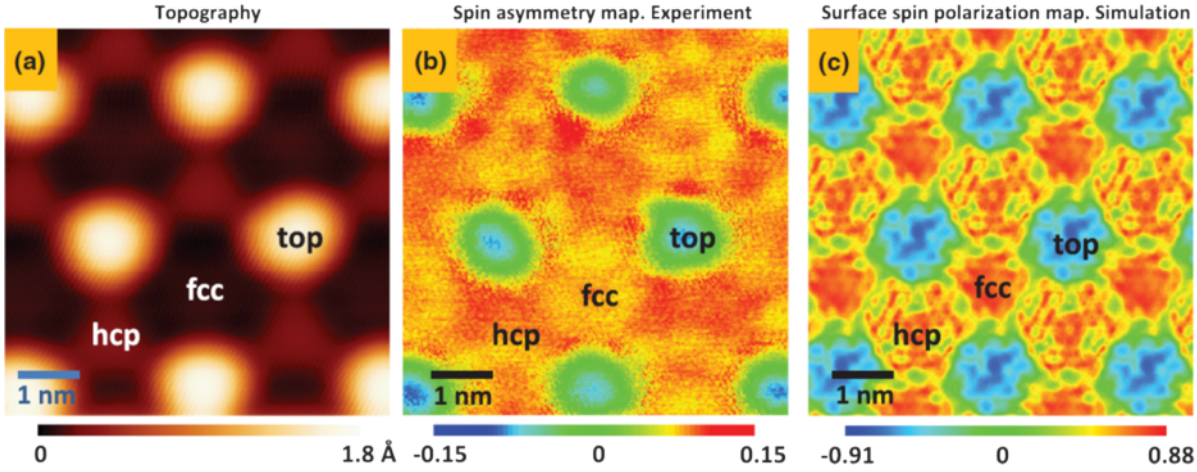

Fig. 6 (colour online). (a) Scanning tunneling microscopy (STM) topography image of a graphene layer adsorbed on the Co/Ir(111) ferromagnetic surface. A strong hybridization (chemisorption) between the p_z atomic orbitals of C and the d-states of Co occurs at the fcc and hcp sites which appear darker in the experimental image. The top sites that appear brighter in the STM image weakly interact (physisorption) with the Co/Ir(111) surface. (b) The experimental and (c) the simulated spin polarization of the region shown in (a) reveals the inversion of the spin polarization between the top sites and fcc/hcp sites. Note that the strongly interacting fcc and hcp sites show also an inversion of the spin polarization with respect to the ferromagnetic Co/Ir(111) surface, while the weakly interacting top sites preserve the spin polarization of the magnetic surface underneath graphene. Interestingly, the panels (b) and (c) define a magnetic Moiré pattern of the graphene/Co/Ir(111) system for an applied bias voltage of -1.0 V. Reprinted with permission from [15]. Copyright 2013 IOP Publishing Ltd.

surements can directly detect with high sensitivity and submolecular resolution the spin polarization above the magnetic hybrid molecular–metallic systems. In Figure 5b, we present the experimental spin-dependent height maps from which we can directly deduce the spin polarization above the adsorbed H_2Pc molecules and ferromagnetic iron layers in a given energy interval. Although the H_2Pc adsorbs in different orientations, it can be easily seen that above all the molecular sites an inversion of the spin polarization occurs with respect to the clean ferromagnetic iron layer surrounding the molecule [14].

Interestingly, the inversion of the spin polarization above organic materials with respect to the ferromagnetic substrate underneath has been observed for other organic materials as graphene when it adsorbs onto ferromagnetic surfaces. In particular, our recent experimental and theoretical investigations of graphene adsorbed on the ferromagnetic monolayer Co/Ir(111) substrate showed the presence of a Moiré pattern (see Fig. 6a) which arises due to the site-dependent strong chemisorption or physisorption type interactions. As depicted in Figure 6a, depending on the specific position of the substrate metallic atoms with respect to the carbon atoms, some graphene regions are called "fcc" and "hcp" sites while other regions are referred as "top" sites (see definition in [15, 33]). Characteristic for the graphene/Co/Ir(111) system is that at the fcc and hcp sites a strong hybridization (chemisorption) between the out-of-plane orbitals of carbon and metallic states take place, while at the top sites only a weak van der Waals (physisorption) type interaction occurs.

The different nature of the bonding mechanisms (i. e. chemisorption or physisorption) at the specific fcc, hcp, and top sites of graphene adsorbed onto the ferromagnetic Co/Ir(111) substrate influences strongly the effective local spin polarization. At the chemisorbed fcc and hcp sites the spin polarization is inverted with respect to the ferromagnetic cobalt layer. On the contrary, the physisorbed top sites preserve the spin polarization of the magnetic surface underneath graphene due to a π–d spin-unbalanced interaction occurring between the graphene π-orbitals and the ferromagnetic d-states of the metal (see Fig. 6b and Fig. 6c). To conclude this section, we have presented how the understanding of the spin polarization above hybrid molecular–ferromagnetic metal systems can be used to gain knowledge about more complex hybrid organic materials as graphene adsorbed onto a ferromagnetic substrate.

1.5. Magnetic Hardening at the Hybrid Organic–Ferromagnetic Interface

In practical applications based on molecular spintronic devices, the spin polarization discussed in the previous section determines the efficiency of the spin polarized current injected from the hybrid interface. Nevertheless, another challenging issue that has to be solved is how the magnetic properties of the underlying metal atoms like magnetic exchange couplings and magnetization direction (spin–orbit interactions) can be specifically modified due to their interaction with organic materials.

We recently addressed this question by performing concept theoretical studies of adsorbed π-conjugated biplanar organic molecules onto ferromagnetic surfaces [6, 41]. As an instructive example, in the following we will shortly discuss the interaction between the paracyclophane (PCP) molecule with a ferromagnetic monolayer of iron on a W(110) substrate. The

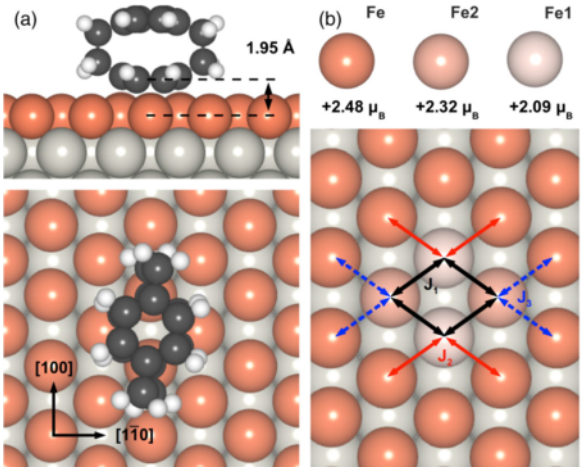

Fig. 7 (colour online). (a) Ground-state adsorption geometry of the paracyclophane (PCP) molecule adsorbed on the Fe/W(110) surface. (b) Top view of four Fe atoms that hybridize with the lower ring of the PCP molecule. The Fe1 is directly below a carbon atom while the Fe2 is under a C–C bond. This leads to a slightly different Fe–C interaction reflected by slightly different magnetic moments for the Fe1 and Fe2 atoms as well as magnetic exchange constants J describing the Fe–Fe magnetic interactions. The magnetic moment of the clean Fe surface atom is also specified. Reprinted with permission from [41]. Copyright 2011 IOP Publishing Ltd.

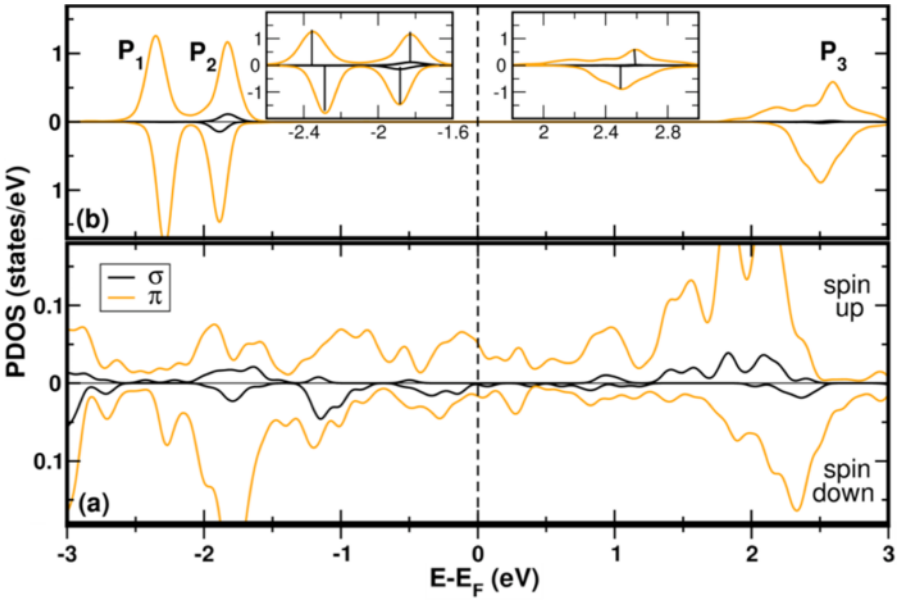

Fig. 8 (colour online). Projected density of states (DOS) at the molecular site expressed in terms of the σ ($s + p_x + p_y$) and π (p_z) type molecular-like orbitals of the lower (a) and the upper (b) ring of the PCP molecule in its ground-state on the Fe/W(110) surface. The lower ring binds to the substrate by chemical bonds and in consequence broad spin-polarized hybrid molecule–surface bands are formed. In contrast, the PDOS for the upper ring shows distinct sharp spin-split molecular-like features. Importantly, the spin degeneracy of the PCP molecular orbitals in gas phase is lifted due to the interaction with the magnetic surface leading to an exchange splitting of 65 meV for the occupied PDOS features at -2.5 eV (P1 peak), 57 meV for the occupied P2 peak, and an exchange splitting of 88 meV for the unoccupied P3 one at 2.5 eV. Reprinted with permission from [41]. Copyright 2011 IOP Publishing Ltd.

choice of the PCP molecule is motivated by its molecular structure: it consists of two benzene-like rings that form a columnar π-conjugated electronic structure connected by two pairs of two sp^3 hybridized carbon atoms.

Our simulations showed that the molecule chemisorbs with a 6π-aromatic benzene-like ring (hereafter denoted as the lower ring) onto the ferromagnetic iron surface, while the other 6π-aromatic benzene-like ring (hereafter denoted as the upper ring) points towards the vacuum interface (see Fig. 7a).

Due to its specific columnar structure, the molecule–substrate interaction leads to hybrid electronic states with very different character at each benzene-like ring. The lower ring shows broad hybrid molecular–metallic bands (see Fig. 8a) due to a strong hybridization between the orbitals of carbon and iron atoms. On the contrary, the upper ring exhibits sharp hybrid electronic states (see Fig. 8b) that were previously known for physisorbed molecules only [6]. We note that sharp spin-split molecular-like electronic features at the molecular site of the upper ring are required for obtaining well-defined spin-filter functionalities [42].

Since the lower ring strongly chemisorbs on four iron atoms (see Fig. 7), we have also calculated several magnetic configurations for which all or some iron atoms underneath the molecule are oriented antiferromagnetically with respect to the clean surface ferromagnetic atoms. By using the differences in the total energies of these magnetic configurations and by applying a Heisenberg model, we evaluated the magnetic exchange constants J describing the coupling strength of the iron–iron magnetic interactions.

One of the most important result of our calculations is that J_1 (15.65 meV) describing the magnetic exchange interactions between the iron atoms below the PCP molecule is drastically increased as compared to that of the clean iron surface atoms J_S (5.42 meV). Therefore, the PCP molecule together with hybridized iron atoms below can be considered as a local molecular-based magnetic unit embedded within the ferromagnetic substrate. Note also that J_2

(5.84 meV) and J_3 (5.17 meV) between the iron atoms forming the local magnetic molecular unit and the neighboring clean iron surface atoms are slightly larger and slightly smaller than J_S (5.42 meV). Furthermore, by including the spin–orbit coupling into the calculations, our study demonstrated that the local molecular-based magnetic unit has a more stable magnetization direction as compared to the one of the iron atom of the clean surface.

Therefore,

(i) the large increase of the magnetic exchange interaction between the magnetic atoms binding directly to the PCP molecule and
(ii) the magnetization direction stabilization of the molecular-based magnetic unit lead to an enhanced barrier for the magnetization switching with respect to the clean iron surface and consequently a magnetic hardening effect [41].

At this point, we mention that the interaction between phenalenyl derivatives with cobalt ferromagnetic surfaces leads to a strong decoupling (magnetic softening) of the local molecular-based magnetic unit from its surrounding magnetic electrode. The magnetic softening effect has been successfully implemented in molecular spintronic devices [6].

2. Conclusions

In this article, we presented an overview of magnetic effects arising at hybrid interfaces when organic materials containing π-electrons interact with ferromagnetic surfaces. Our theoretical studies showed that the density functional theory provides a framework with predictive power where a realistic understanding of these organic–metallic hybrid systems can be expected. Beside this, our studies demonstrated the decisive role played by the van der Waals forces in correctly describing the interaction between π-conjugated organic materials and magnetic surfaces. Furthermore, we showed how the strong hybridization between the magnetic d-states of the metal with the p_z-electrons that initially form the π-orbitals in organic materials influences the spin polarization, the magnetic exchange coupling, and the magnetization direction at hybrid organic–ferromagnetic interfaces. In particular, we shortly reviewed how a detailed understanding gained through theoretical simulations allows us to tailor the magnetic properties of hybrid interfaces. This knowledge can be of technological interest and used to design future spintronic devices based on organic molecules.

[1] C. Joachim, J. K. Gimzewski, and A. Aviram, Nature **408**, 541 (2000).
[2] A. Nitzan and M. A. Ratner, Science **300**, 1384 (2003).
[3] I. Diez-Perez, J. Hihath, Y. Lee, L. Yu, L. Adamska, M. A. Kozhushner, I. I. Oleynik, and N. Tao, Nature Chem. **1**, 635 (2009).
[4] A. H. Flood, J. F. Stoddart, D. W. Steuerman and J. R. Heath, Science **306**, 2055 (2004).
[5] S. Kubatkin, A. Danilov, M. Hjort, J. Cornil, J. L. Bredas, N. Stuhr-Hansen, P. Hedegard, and T. Bjørnholm, Nature **425**, 698 (2003).
[6] K. V. Raman, A. M. Kamerbeek, A. Mukherjee, N. Atodiresei, T. K. Sen, P. Lazic, V. Caciuc, R. Michel, D. Stalke, S. K. Mandal, S. Blügel, M. Münzenberg, and J. S. Moodera, Nature **493**, 509 (2013).
[7] A. J. Drew, J. Hoppler, L. Schulz, F. L. Pratt, P. Desai, P. Shakya, T. Kreouzis, W. P. Gillin, A. Suter, N. A. Morley, V. K. Malik, A. Dubroka, K. W. Kim, H. Bouyanfif, F. Bourqui, C. Bernhard, R. Scheuermann, G. J. Nieuwenhuys, T. Prokscha, and E. Morenzoni, Nature Mat. **8**, 109 (2009).
[8] C. Barraud, P. Seneor, R. Mattana, S. Fusil, K. Bouzehouane, C. Deranlot, P. Graziosi, L. Hueso, I. Bergenti, V. Dediu, F. Petroff, and A. Fert, Nature Phys. **6**, 615 (2010).
[9] M. Cinchetti, K. Heimer, J.-P. Wüstenberg, O. Andreyev, M. Bauer, S. Lach, C. Ziegler, Y. Gao, and M. Aeschlimann, Nature Mat. **8**, 115 (2009).
[10] S. Majumdar, H. S. Majumdar, R. Laiho, and R. Österbacka, New J. Phys. **11**, 13022 (2009).
[11] M. Urdampilleta, S. Klyatskaya, J.-P. Cleuziou, M. Ruben, and W. Wernsdorfer, Nature Mat. **10**, 502 (2011).
[12] L. Bogani and W. Wernsdorfer, Nature Mat. **7**, 179 (2008).
[13] J. Brede, N. Atodiresei, S. Kuck, P. Lazic, V. Caciuc, Y. Morikawa, G. Hoffmann, S. Blügel, and R. Wiesendanger, Phys. Rev. Lett. **105**, 47204 (2010).
[14] N. Atodiresei, J. Brede, P. Lazic, V. Caciuc, G. Hoffmann, R. Wiesendanger, and S. Blügel, Phys. Rev. Lett. **105**, 66601 (2010).
[15] R. Decker, J. Brede, N. Atodiresei, V. Caciuc, S. Blügel, and R. Wiesendanger, Phys. Rev. B **87**, 41403 (2013).

[16] J. B. Neaton, M. S. Hybertsen, and S. G. Louie, Phys. Rev. Lett. **97**, 216405 (2006).
[17] J. M. Garcia-Lastra and K. S. Thygesen, Phys. Rev. Lett. **106**, 187402 (2011).
[18] D. C. Langreth, B. I. Lundqvist, S. D. Chakarova-Kack, V. R. Cooper, M. Dion, P. Hyldgaard, A. Kelkkanen, J. Kleis, L. Kong, S. Li, P. G. Moses, E. Murray, A. Puzder, H. Rydberg, E. Schröder, and T. Thonhauser, J Phys. Cond. Mat. **21**, 84203 (2009).
[19] I. Fleming, Frontier Orbitals and Organic Chemical Reactions, John Wiley & Sons, London 1978.
[20] M. C. Lennartz, N. Atodiresei, L. Mueller-Meskamp, S. Karthäuser, R. Waser, and S. Blügel, Langmuir **25**, 856 (2009).
[21] M. C. Lennartz, V. Caciuc, N. Atodiresei, S. Karthäuser, and S. Blügel, Phys. Rev. Lett. **105**, 66801 (2010).
[22] J. K. Nørskov, Rep. Prog. Phys. **53**, 1253 (1990).
[23] P. Hohenberg and W. Kohn, Phys. Rev. **136**, B864 (1964).
[24] D. M. Ceperley and B. J. Alder, Phys. Rev. Lett. **45**, 566 (1980).
[25] J. P. Perdew, K. Burke, and M. Ernzerhof, Phys. Rev. Lett. **77**, 3865 (1996).
[26] M. Dion, H. Rydberg, E. Schröder, D. C. Langreth, and B. I. Lundqvist, Phys. Rev. Lett. **92**, 246401 (2004).
[27] K. Burke, J. Chem. Phys. **136**, 150901 (2013).
[28] P. Lazic, M. Alaei, N. Atodiresei, V. Caciuc, R. Brako, and S. Blügel, Phys. Rev. B **181**, 45401 (2010).
[29] S. Grimme, J. Comput. Chem. **27**, 1787 (2006).
[30] J. Klimes and A. Michaelides, J. Chem. Phys. **137**, 120901 (2012).
[31] N. Atodiresei, V. Caciuc, P. Lazic, and S. Blügel, Phys. Rev. Lett. **102**, 136809 (2009).
[32] C. Busse, P. Lazic, R. Djemour, J. Coraux, T. Gerber, N. Atodiresei, V. Caciuc, R. Brako, A. T. N'Diaye, S. Blügel, J. Zegenhagen, and T. Michely, Phys. Rev. Lett. **107**, 36101 (2011).
[33] H. Harutyunyan, M. Callsen, T. Allmers, V. Caciuc, S. Blügel, N. Atodiresei, and D. Wegner, Chem. Commun. **49**, 5993 (2013).
[34] N. Atodiresei, V. Caciuc, P. Lazic, and S. Blügel, Phys. Rev. B **84**, 172402 (2011).
[35] V. Caciuc, M. C. Lennartz, N. Atodiresei, S. Karthäuser, and S. Blügel, Nanotech. **22**, 145701 (2011).
[36] J. Kanamori and K. Terakura, J. Phys. Soc. Japan **70**, 1433 (2001).
[37] N. Atodiresei, P. H. Dederichs, Y. Mokrousov, L. Bergqvist, G. Bihlmayer, and S. Blügel, Phys. Rev. Lett. **100**, 117207 (2008).
[38] S. Fahrendorf, N. Atodiresei, C. Besson, V. Caciuc, F. Matthes, S. Blügel, P. Kögerler, D. E. Bürgler, and C. M. Schneider, Nature Commun. **4**, 2425 (2013).
[39] F. Meier, L. Zhou, J. Wiebe, and R. Wiesendanger, Science **320**, 82 (2008).
[40] R. Wiesendanger and H.-J. Güntherodt, Phys. Rev. Lett. **65**, 247 (1990).
[41] M. Callsen, V. Caciuc, N. Kiselev, N. Atodiresei, and S. Blügel, Phys. Rev. Lett. **111**, 106805 (2013).
[42] J. Schwöbel, Y. Fu, J. Brede, A. Dilullo, G. Hoffmann, S. Klyatskaya, M. Ruben, and R. Wiesendanger, Nature Commun. **3**, 953 (2012).